Bi-exponential diffusion analysis in normal prostate and prostate cancer: transition zone and peripheral zone considerations

Thiele Kobus[1,2], Andriy Fedorov[1], Clare Tempany[1], Robert Mulkern[3], Ruth Dunne[1], and Stephan E. Maier[1]

[1]Radiology, Brigham and Women's Hospital, Boston, Massachusetts, United States, [2]Radiology, Radboud UMC, Nijmegen, Netherlands, [3]Radiology, Children's Hospital, Boston, Massachusetts, United States

Target audience: Clinicians and scientists involved with MR imaging of the prostate.

Purpose: Prostate diffusion-weighted imaging (DWI) is typically performed using a small number of b-values under 1400 s/mm^2 with apparent diffusion coefficients (ADCs) calculated assuming mono-exponential decays. Over an extended range of b-values, bi-exponential fits better characterize the signal decay and offer additional tissue characterization. Especially for b-factors > 2000 s/mm^2, the bi-exponential model has more information content than mono-exponential or kurtosis models[1]. Cancer detection in the transition zone (TZ) of the prostate remains challenging. Promising results have been published using the parameters obtained from bi-exponential fits to differentiate TZ tumors from normal tissue[2]. Here, we assess tumors originating from the peripheral zone (PZ) and TZ separately and evaluate the performance of the bi-exponential model to differentiate these tumors from normal tissue.

Materials and methods: *Image acquisition*: In this IRB approved prospective study, 38 patients with (suspected) prostate cancer who did not receive prior radiation- or hormonal therapy, underwent a clinical multi-parametric MR exam. The MR exam was expanded with an extended b-factor DWI sequence. All examinations were performed on a 3T MR-system (GE Discovery MR750) and an endorectal coil was combined with pelvic phased array coils for signal reception. The clinical MR protocol consisted of high-resolution T2-weighted imaging in three orthogonal directions, T1-weighted imaging, clinical DWI (b=500 and 1400 s/mm^2) and DCE-MRI. The extended b-factor DWI was measured with 15 b-factors equally spaced from b=0 to 3500 s/mm^2 and with three orthogonal diffusion-sensitization directions. Image parameters were: TE 99-102 ms, TR 4000ms, slice thickness 5 mm, FOV 280x280 mm, 64x64 acquisition matrix, 1.1x1.1 mm spatial resolution after reconstruction. The signal intensity of the trace images, S(b), versus b-factor was fit to a bi-exponential decay using a non-linear least square fitting (Levenberg-Marquardt) algorithm. In the equation, $S(b) = S_0\left(f_{fast}e^{-bADC_{fast}} + f_{slow}e^{-bADC_{slow}}\right)$, S_0 is the fitted signal intensity for b=0, ADC_{fast} and ADC_{slow} represent the fast and slow apparent diffusion components, and f_{fast} and f_{slow} are the fractions of the fast and slow components ($f_{slow}+f_{fast}=1$). The fitting procedure was implemented in 3D Slicer[3] and three parameter maps (ADC_{slow}, ADC_{fast} and f_{slow}) were generated (Fig 1. C-E).

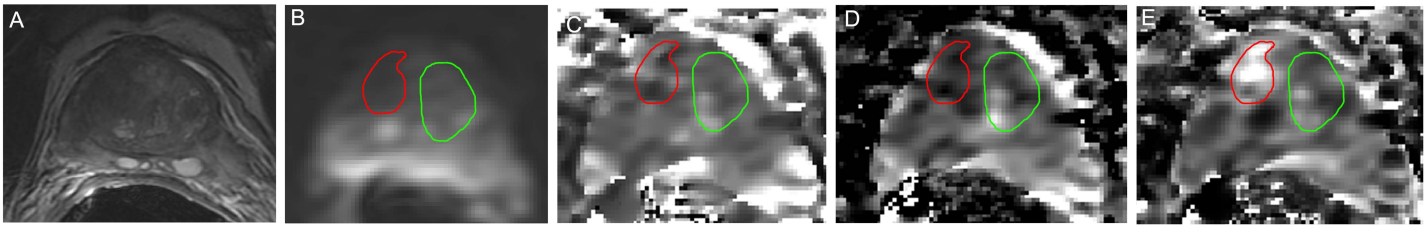

Figure 1. A) T2-weighted image of a 77-year old patient with a PSA level of 13.8 ng/mL and Gleason score 4+3 on biopsy. B) b=0 image with red ROI indicating tumor-suspicious area and green ROI normal appearing TZ. C) Map of ADC_{fast}. D) Map of ADC_{slow} E) Map of f_{slow}

Image processing: One radiologist evaluated all clinical MR images, except the extended b-factor DW images, and indicated normal appearing PZ, normal appearing TZ and if tumor suspicious region(s) was/were present, the index lesion. In the cases where the radiologist indicated a different index lesion than the clinical MR report, a consensus reading with a second radiologist was performed. Regions of interest (ROIs) were drawn in normal PZ & TZ and tumor TZ & PZ tissue in 3D Slicer on the b=0 image of the extended b-factor DWI images (Fig 1B). Voxels with either a negative ADC_{slow} or $ADC_{fast} \geq 4000$ mm^2/s were excluded from the ROIs. Next, the mean ADC_{fast}, ADC_{slow} and f_{slow} were determined per ROI. The means of the four tissues were compared with ANOVA and a Tukey's post hoc-test.

Results: An index lesion was indicated by the radiologist in 24 patients (13 PZ and 11 TZ); in the other patients only ROIs of normal appearing tissue were included. In all patients the quality of the extended b-factor images was sufficient to obtain reliable parameter maps (Fig 1). For all three parameters, the means (Table) of normal PZ and normal TZ differed significantly from tumor tissue in both PZ and TZ. For f_{slow} there was also a difference between normal PZ and TZ (Fig 2).

	ADC_{fast} (x 10^{-3} mm^2/s)	ADC_{slow} (x 10^{-3} mm^2/s)	f_{slow}	ROI vol. (cm^3)
PZ	2.83±0.19	0.54±0.10	0.18±0.05	0.87±0.38
Tumor PZ	2.51±0.28	0.41±0.09	0.33±0.07	2.00±1.25
TZ	2.76±0.25	0.52±0.07	0.27±0.05	0.61±0.38
Tumor TZ	2.47±0.43	0.40±0.09	0.39±0.12	0.61±0.31

Means and standard deviations for ADC_{fast}, ADC_{slow}, f_{slow} and ROI volume.

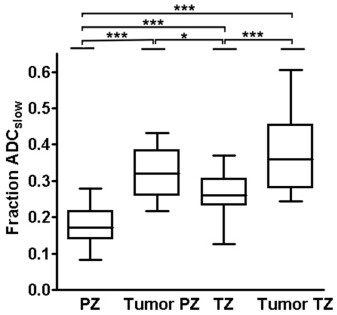

*Figure 2. Boxplot of f_{slow}, (whiskers indicate min and max) *** p<0.001, * p<0.05*

Discussion and conclusion: Our findings are in line with the findings of Liu et al[2], who found significant decreases in ADC_{fast}, ADC_{slow} and f_{fast} in TZ tumors and Maier et al[4] who showed a decrease in f_{fast} in PZ tumors. Because we included normal and tumor tissue from both prostate zones, we could compare tumors arising in the TZ from PZ tumors. We did not find any differences for ADC_{fast}, ADC_{slow} and f_{slow} between the two groups of tumors. In the normal PZ and TZ we found significant differences between the two zones for f_{slow}. Although both ADC_{fast} and ADC_{slow} decreased in cancer, there was a larger relative increase of f_{slow}, which might represent the occupation of the luminal space by tumor cells. A validation based on histopathology is necessary to test the clinical implication of our results, especially of interest is whether this technique can be used to better characterize TZ tumors, where the performance of mono-exponentially obtained ADC-values is inadequate.

References: 1. Bourne, Panagiotaki, Bongers et al. Information Theoretic Ranking of Four Models of Diffusion Attenuation in Fresh and Fixed Prostate Tissue Ex Vivo, Mag Res Med 2013, 1418-1426 **2**. Liu, Zhou, Peng et al. Differentiation of central gland prostate cancer from benign. Magn Reson Imaging 2013, 1318-1324. **3**. Fedorov, Beichel, Kalpathy-Cramer et al. 3D Slicer as an Image Computing Platform for the Quantitative Imaging Network. Magn Reson Imaging. 2012, 1323-41. **4**. Maier, Tang, Panych et al. Non-monoexponential Diffusion Signal Decay in Prostate Cancer - ISMRM 2011 - 1053

Acknowledgements: NIH CA160902, EB010195, EB015898, P41EB015898, CA180918, ERC grant PIOF-GA-2012-331813, KWF 2013-5861